Identification of CD157-Positive Vascular Endothelial Stem Cells in Mouse Retinal and Choroidal Vessels: Fluorescence-Activated Cell Sorting Analysis

Taku Wakabayashi,[1–3,*] Hisamichi Naito,[1,4,*] Tomohiro Iba,[1,4] Kohji Nishida,[2,5] and Nobuyuki Takakura[1]

[1]Department of Signal Transduction, Research Institute for Microbial Diseases, Osaka University, Suita, Osaka, Japan
[2]Department of Ophthalmology, Osaka University Graduate School of Medicine, Suita, Osaka, Japan
[3]Wills Eye Hospital, Mid Atlantic Retina, Thomas Jefferson University, Philadelphia, Pennsylvania, United States
[4]Department of Vascular Molecular Physiology, Kanazawa University Graduate School of Medical Science, Takaramachi, Kanazawa, Ishikawa, Japan
[5]Integrated Frontier Research for Medical Science Division, Institute for Open and Transdisciplinary Research Initiatives, Osaka University, Osaka, Suita, Japan

Correspondence: Taku Wakabayashi, Department of Ophthalmology, Osaka University Graduate School of Medicine, 2-2 Yamadaoka, Suita, Osaka 565-0871, Japan; taku.wakabayashi@gmail.com. Nobuyuki Takakura, Department of Signal Transduction, Research Institute for Microbial Diseases, Osaka University, 3-1 Yamada-oka, Suita, Osaka 565-0871, Japan; ntakaku@biken.osaka-u.ac.jp.

TW and HN contributed equally to this work.

Received: August 23, 2021
Accepted: March 27, 2022
Published: April 8, 2022

Citation: Wakabayashi T, Naito H, Iba T, Nishida K, Takakura N. Identification of CD157-positive vascular endothelial stem cells in mouse retinal and choroidal vessels: Fluorescence-activated cell sorting analysis. *Invest Ophthalmol Vis Sci.* 2022;63(4):5. https://doi.org/10.1167/iovs.63.4.5

Purpose. CD157 (also known as Bst1) positive vascular endothelial stem cells (VESCs), which contribute to vascular regeneration, have been recently identified in mouse organs, including the retinas, brain, liver, lungs, heart, and skin. However, VESCs have not been identified in the choroid. The purpose of this study was to identify VESCs in choroidal vessels and to establish the protocol to isolate retinal and choroidal VESCs.

Methods. We established an efficient protocol to create single-cell suspensions from freshly isolated mouse retina and choroid by enzymatic digestion using dispase, collagenase, and type II collagenase. CD157-positive VESCs, defined as $CD31^+CD45^-CD157^+$ cells, were sorted using fluorescence-activated cell sorting (FACS).

Results. In mouse retina, among $CD31^+CD45^-$ endothelial cells (ECs), 1.6 ± 0.2% were CD157-positive VESCs, based on FACS analysis. In mouse choroid, among $CD31^+CD45^-$ ECs, 4.5 ± 0.4% were VESCs. The CD157-positive VESCs generated a higher number of EC networks compared with CD157-negative non-VESCs under vascular endothelial growth factor (VEGF) in vitro cultures. The EC network area, defined as the ratio of the CD31-positive area to the total area in each field, was 4.21 ± 0.39% (retinal VESCs) and 0.27 ± 0.12% (retinal non-VESCs), respectively ($P < 0.01$). The EC network area was 8.59 ± 0.78% (choroidal VESCs) and 0.14 ± 0.04% (choroidal non-VESCs), respectively ($P < 0.01$). The VESCs were located in large blood vessels but not in the capillaries.

Conclusions. We confirmed distinct populations of CD157-positive VESCs in both mouse retina and choroid. VESCs are located in large vessels and have the proliferative potential. The current results may open new avenues for the research and treatment of ocular vascular diseases.

Keywords: vascular endothelial stem cells, VESCs, endothelial cells, CD157, bst1, flow cytometry, fluorescence-activated cell sorting, single-cell suspension, angiogenesis, retina, choroid, immunostaining

Blood vessels in the retina and choroid provide oxygen and nourishment to the inner and outer layers of the retina, respectively.[1,2] Vascular endothelial cells (ECs) that line the inner surface of retinal and choroidal blood vessels are essential for the maintenance of retinal homeostasis.[3,4] In adults with established vascular structures, most ECs are quiescent but have the ability to proliferate and form new blood vessels under hypoxic conditions in a process known as angiogenesis.[5] There has been a long-standing debate regarding the cellular sources of the initiation and progression of angiogenesis. Cellular sources that have been proposed include circulating endothelial progenitor cells (EPCs) derived from bone marrow (BM), proliferation of resident mature ECs in a stochastic (random) manner, and specialized vascular endothelial stem cells (VESCs) residing within the blood vessels, which proliferate in a hierarchical manner.[6–8] Although the role of EPCs in angiogenesis has been extensively studied over the last 2 decades, BM-derived EPCs rarely engraft and differentiate into ECs, indicating a minor or no contribution to angiogenesis.[9–11] In contrast, recent studies have suggested the existence of specific ECs within blood vessels responsible for angiogenesis in adults.[12,13]

Endothelial colony-forming cells (ECFCs), which form a subset of endothelial cell progenitors that show higher proliferative capacity than mature endothelial cells, are

responsible for angiogenesis.[14,15] ECFCs possess VESC properties, such as clonal proliferative potential and vascular regeneration potential in vivo. Hoechst 33342 staining negative vascular ECs with the side population (SP) phenotype (EC-SP), defined as VE-cadherin^{+}CD31^{+}CD45^{-}Hoechst^{low}, have also been regarded as vessel-residing VESCs in the retina and choroid.[16,17] However, the lack of unique and robust markers to prospectively identify ECFC and EC-SP in vivo has limited the recognition of VESCs until recently.

Recently, we identified CD157, which is also known as BM stromal antigen-1 (Bst1), as a marker of VESCs in adult mouse blood vessels.[18] This marker was discovered based on a microarray analysis of EC-SP cells. Among the 24,321 genes analyzed, CD157 was highly expressed in EC-SP but not in most other ECs. CD157-positive VESCs reside in the large blood vessels of numerous mouse organs. Genetic lineage tracing in mouse livers revealed that VESCs proliferated and sequentially regenerated functional blood vessels from large vessels to capillaries in response to acute damage or as part of normal physiological turnover. In addition, single VESC transplantation experiments generated three-dimensional functional blood vessels in vivo, reflecting their stem cell properties. The CD157-positive VESCs were not from the BM or mesenchymal lineage. Although we previously identified VESCs in the retina, CD157-positive VESCs in the choroid have not been investigated. Moreover, no previous study has described detailed methods for isolating CD157-positive VESCs from the retina and choroid using fluorescence-activated single-cell sorting (FACS) in mice.

In the present study, we established a protocol to isolate ECs from mouse retina and choroid by enzymatic tissue digestion followed by FACS, and identified CD157-positive VESCs in both the retina and choroid. We also described the location and an in vitro culture of VESCs that showed the proliferative potential to form EC networks.

Methods

Mice

Female C57BL/6J mice aged 8 to 12 weeks were purchased from Japan SLC (Shizuoka, Japan). The use of CD157 knockout (CD157-KO) mice has been reported elsewhere.[19] All animal experiments were conducted in accordance with the ARVO Animal Statement for the Use of Animals in Ophthalmic and Vision Research.

Isolation of Adult Mice Retina and Choroid

C57BL/6J mice were euthanized by cervical dislocation under anesthesia. The eyes were enucleated and submerged in ice-cold cell suspension buffer containing 4% (v/v) fetal bovine serum (FBS; Sigma-Aldrich, cat. #172012-500ML) in PBS (−) (Fig. 1A). The cornea, lens, iris, and vitreous humor were removed by circumferential cutting above the ora serrata, creating an eyecup. The sensory retina was peeled away from the eyecup and transferred to an ice-cold cell suspension buffer (Fig. 1B). The remaining eyecup contained the choroid and sclera. The choroid was separated from the sclera using a small laboratory spoon/spatula and transferred to an ice-cold cell suspension buffer (see Fig. 1B).

Preparation of Enzymes for Single-Cell Suspension

Dispase (Gibco, cat. #17105-041), collagenase (Wako, cat. #034-22363), and type II collagenase (Worthington, cat. #LS004176) solutions were prepared. For the dispase solution (for the first stage of enzymatic dissociation), we prepared 2.4 U/mL of stock solution in 10 mL of PBS (−) and stored it at −20°C. Before the experiments, we added an equal volume of cell suspension buffer (noted above) and created a solution with the final concentration of 1.2 U/mL. We prewarmed at 37°C for 20 minutes before usage. For the collagenase solution (for the second stage of enzymatic dissociation), we added 20 mg of collagenase, 18 µL of $CaCl_2$ (1M; Honeywell Fluka, cat. #21114-1L), and 6.6 µL of $MgCl_2$ (1M; Sigma-Aldrich, cat. #M1028-100ML) to 20 mL of cell suspension buffer. Because this solution could not be stored, it was freshly prepared for each experiment. The collagenase solution with a final concentration of 1 mg/mL was prewarmed at 37°C for 20 minutes before its usage. For the type II collagenase solution (in the third stage of enzymatic dissociation), we added 20 mg of type II collagenase, 18 µL of $CaCl_2$, and 6.6 µL of $MgCl_2$ to 20 mL of cell suspension buffer. This solution also could not be stored and was freshly prepared in each experiment. The type II collagenase solution with a final concentration of 1 mg/mL was prewarmed at 37°C for 20 minutes before usage. $CaCl_2$ is critical for activating collagenase activity.

Creating a Single-Cell Suspension

The retinas and choroids were each transferred to a 50-mL conical tube (Falcon, cat. #352070) (Fig. 1C). Next, 20 mL of dispase solution was added to the 50-mL conical tube, including the retina or choroid. In the first stage of enzymatic dissociation, the solution in the 50-mL conical tube was mixed by shaking it up and down 3 times without creating bubbles. The tubes were then incubated in a water bath for 5 minutes at 37°C (Fig. 1D). After 5 minutes, the conical tube was centrifuged at 330 × *g* for 3 minutes at 4°C, and the supernatants were discarded. In the second stage of enzymatic dissociation, the retinal and choroidal cell pellets were resuspended in 20 mL of collagenase solution. The solution in the 50-mL conical tube was mixed again by shaking up and down 3 times without generating bubbles, and then incubated in a water bath for 7 minutes at 37°C. After 7 minutes (see Fig. 1D), the conical tube was centrifuged at 330 × *g* for 3 minutes at 4°C, and the supernatants were discarded. In the third stage of enzymatic dissociation, the retinal or choroidal cell pellets were resuspended in 20 mL of type II collagenase solution. The solution in the 50-mL conical tube was mixed by shaking up and down 3 times without forming bubbles, and then incubated in a water bath for 7 minutes at 37°C (see Fig. 1D). Next, a 40-µm cell strainer was placed on a new 50-mL conical tube, and the retinal and choroidal digests were decanted through the strainer (Fig. 1E). The 50-mL conical tube containing the retinal and choroidal digests was then centrifuged at 330 × *g* for 3 minutes at 4°C. The supernatant was discarded, and the retinal and choroidal cell pellets were resuspended in 1 mL of ACK lysing buffer (Lonza, cat. #10-548E) for red blood cell lysis. The cells were subsequently mixed using a P1000 pipette, and the cell suspension was incubated for 1 minute at room temperature. Then, 20 mL of cell suspension buffer was added, and the 50-mL conical tube was centrifuged at

Investigative Ophthalmology & Visual Science

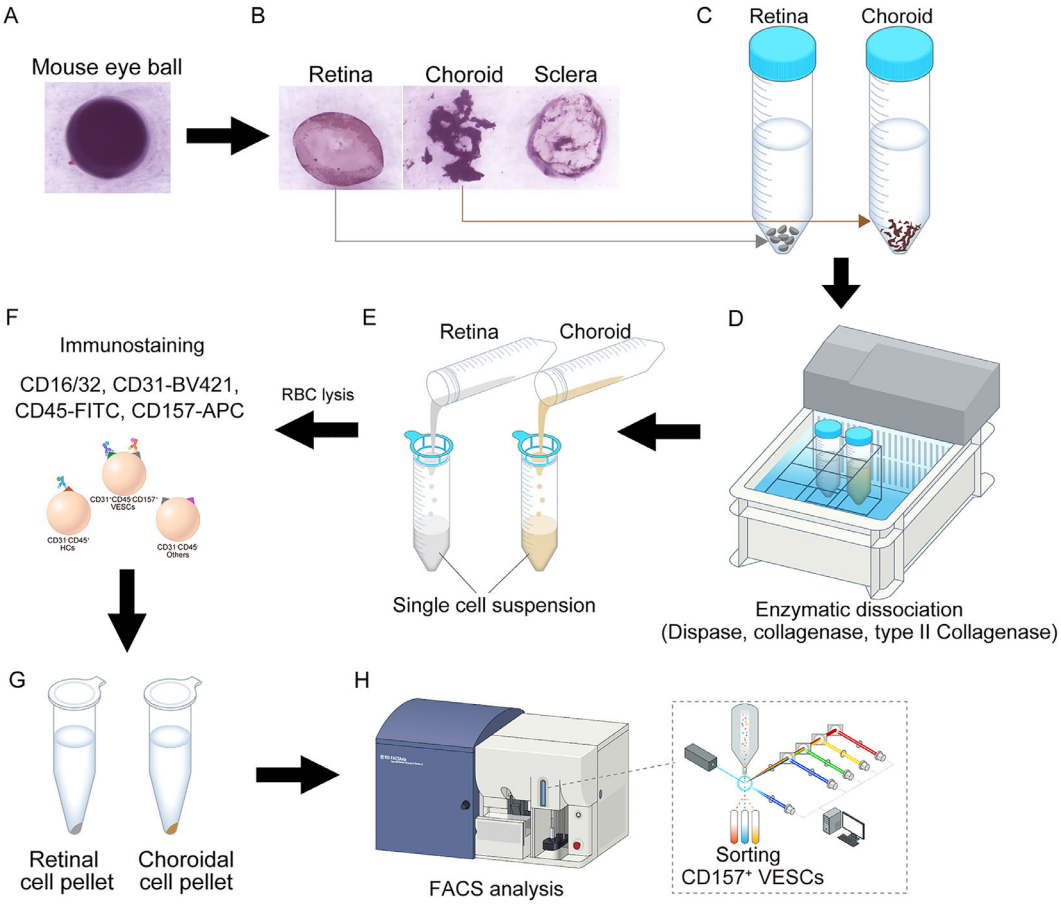

Figure 1. Schema of preparation of single-cell suspensions and isolation of CD157-positive VESCs from mouse retina and choroid. (**A**) The mouse eyeballs were removed. (**B**) The sensory retina was peeled away from the eyecup, and the choroid was separated from the sclera using a small laboratory spoon/spatula. (**C**) The retina and choroid were transferred to a 50-mL conical tube. (**D**) The retina or choroid was dissolved in 20 mL of dispase solution (in the 50-mL conical tube) and warmed for 5 minutes in a water bath. Each tissue sample was centrifuged and then dissolved in 20 mL of collagenase solution. The sample was warmed for 7 minutes and centrifuged. The same steps were repeated with 20 mL of type II collagenase solution. (**E**) A 40-µm cell strainer was placed on a new 50-mL conical tube, and the tissue digests were passed through the strainer by decanting and then centrifuged again. (**F**) After washing and red blood cell lysis, the single-cell suspension in the 1.5-mL microtube was ready for cell surface staining with CD16/CD32 Fc receptors, CD31-BV421, CD45-FITC, and CD157-APC. (**G**) After washing, the cell pellet was resuspended in 500 µL of cell suspension buffer. A single-cell suspension was finally obtained. (**H**) An FACS sorter equipped with blue, red, yellow, green, and violet lasers (BD, FACS Aria II SORP) was used to sort CD157-positive vascular endothelial stem cells (VESC) and CD157-negative non-VESCs from the retina and choroid.

330 × *g* for 3 minutes at 4°C. The supernatant was discarded, and the retinal and choroidal cell pellets were washed with 1 mL of cell suspension buffer. The cell suspension was then placed in a 1.5-mL microtube (AxyGen, cat. #MCT-150-C), which was then centrifuged at 400 × *g* for 3 minutes at 4°C. The supernatant was discarded, and the cell pellets were resuspended in 500 µL of cell suspension buffer. Finally, a single-cell suspension was obtained. The preparation of single-cell suspensions was completed within 1 hour.

Immunostaining of Single-Cell Suspension

In brief, 0.5 µg of purified rat anti-mouse CD16/CD32 antibody (Fc blocking; clone 2.4G2; BD Biosciences, cat. #553142) was added to the above single-cell suspension to inhibit the non-antigen-specific binding of immunoglobulins to the CD16 and CD32 Fc receptors. The single-cell suspension was distributed into four 1.5-mL microtubes, which were the FACS samples: (CD31-BV421 [2 µl] clone 390; BioLegend, cat. #102423, CD45-FITC [2 µl] clone 30-F11; Thermo Fisher Scientific, cat. #11-0451-85, and CD157-APC [2 µl] clone BP-3; BioLegend, cat. #140208; Fig. 1F), negative unstained cells, single-stained controls, and fluorescence minus one (FMO) controls. The cells were incubated for 15 minutes in the dark on ice, washed twice by adding 1 mL of cell suspension buffer, and then centrifuged at 400 × *g* for 3 minutes at 4°C. The supernatant was aspirated, and 500 µL of cell suspension buffer was added (Fig. 1G). The cells were kept in the dark on ice until the FACS sorting process was conducted.

Isolation of CD157-Positive VESCs by FACS

In brief, 1 µL of propidium iodide (PI; Sigma-Aldrich, cat. #P4170-10MG) was added to the sample, and the sample was passed through a 40-µm cell strainer (Falcon, cat. #352340) to remove cell aggregates. Cell aggregation commonly occurs in the retina, but not in the choroid. An FACS sorter equipped with blue, red, yellow-green, and violet lasers (FACS Aria II SORP; BD; Fig. 1H) was used. An

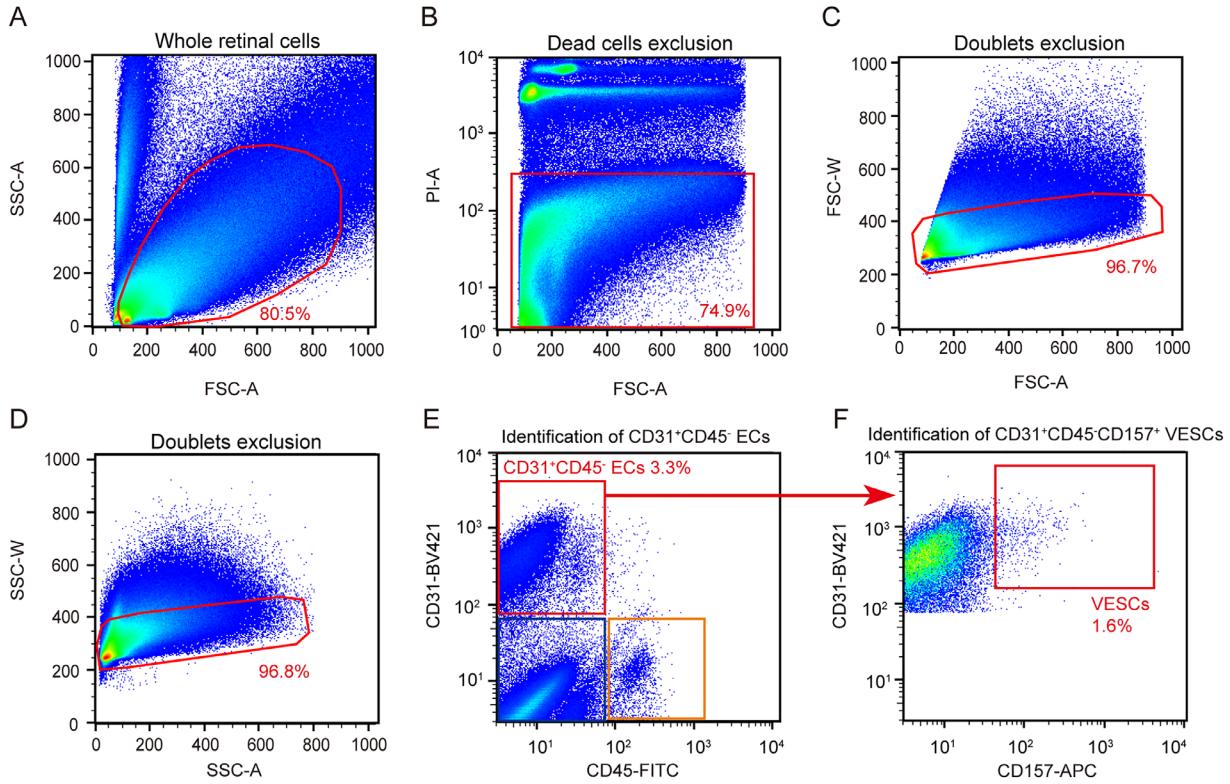

Figure 2. FACS gating strategy for sorting retinal CD157-positive VESCs. Representative FACS plots of the percentage of parent gates for each population. The retinal cell population was selected (**A**), dead cells were excluded (**B**), and doublets were excluded (**C, D**). (**E**) CD31-BV421-A versus CD45-FITC-A dot plot was generated to identify vascular endothelial cells (ECs) positive for the endothelial marker CD31 and negative for the hematopoietic marker CD45 ($CD31^+CD45^-$) in the retina. The proportion of retinal ECs shown in red squares was 3.3% in this experiment. The orange square shows hematopoietic cells ($CD31^+CD45^-$), and the blue squares indicate others ($CD31^-CD45^-$). (**F**) CD31-BV421-A versus CD157-APC-A dot plot was generated to detect CD157-positive vascular endothelial stem cells (VESCs). The proportion of VESCs was 1.6% among all retinal ECs.

85- or 100-µm nozzle was used in the flow cytometry. We ran the sample at a rate of 1.4 to 1.8 and an event rate of 1500 to 2500 events/second. We used an unstained control and a single-stained control to compensate for the FACS machine. The FMO controls were used to set the gates. To analyze the FACS samples (i.e. CD31-BV421, CD45-FITC, and CD157-APC), we generated a forward scatter area (FSC-A) versus a side scatter area (SSC-A) dot plot to select all cells and exclude debris (Fig. 2A). We next generated an FSC-A versus propidium iodide area (PI-A) dot plot to exclude dead cells (Fig. 2B). Next, we generated FSC-A versus forward scatter width (FSC-W; Fig. 2C) and SSC-A versus side scatter width (SSC-W) dot plots to exclude doublets (Fig. 2D). A CD31-BV421-A versus CD45-FITC-A dot plot was generated to identify vascular ECs in the retina (Fig. 2E). CD31-BV421-A versus CD157-APC-A dot plots were generated to detect CD157-positive VESCs (Fig. 2F). We sorted CD157-positive VESCs and CD157-negative vascular ECs into 700 µL of cell suspension buffer in a screwcap microtube (Sarstedt, cat. #72.703.600), which was kept at 4°C. The gates of the CD157-positive VESCs sorting were set based on CD157-FMO controls and validated by the FACS analysis of CD157 KO mouse retina and choroid (Supplementary Fig. S1). We used the "purity sorting mode" to sort the cells. The screwcap microtube containing sorted cells was centrifuged at 400 × *g* for 5 minutes at 4°C and then resuspended in the cell culture medium described below. The FACS sample of the choroid was similarly analyzed (Figs. 3A–F).

In Vitro Culture of CD157-Positive VESCs

One day before sorting and culturing of ECs, OP9 stromal cells (RCB1124, RIKEN cell bank, Tsukuba, Japan) were seeded into 48-well plates (Greiner Bio-One, cat. #677180) so that the OP9 stromal cells would become confluent on the day of the culture. Primary CD157-positive VESCs and CD157-negative ECs were isolated as described above, and 5000 cells/well from the choroid and 2500 cells/well from the retina were plated into 48-well plates for the EC network formation assay. Eight mice (16 eyeballs) were necessary to isolate 5000 and 2500 CD157-positive VESCs from the choroid and the retina, respectively. Cultures were maintained in RPMI (Sigma-Aldrich, cat. #R8758-500ML) supplemented with 10% FBS and 10^{-5} mol/L 2-mercaptoethanol (Gibco, cat. #21985023). The plate was incubated at 37°C in a 5.0% CO_2 atmosphere. VEGF165 (10 ng/mL; PeproTech, cat. #100-20) was added to the cultures every 3 days. The cells were fixed for immunostaining with CD31 after 10 days.[16,17]

Immunostaining of EC Networks In Vitro

In immunostaining with CD31, anti-CD31 mAb (BD Biosciences, cat. #553370) was used, and biotin-conjugated polyclonal anti-rat Ig (Dako, Glostrup, Denmark) was used as secondary antibodies. Biotinylated secondary antibodies were developed using ABC kits (Vector Laboratories, Burlingame, CA, USA). The samples were visualized using an

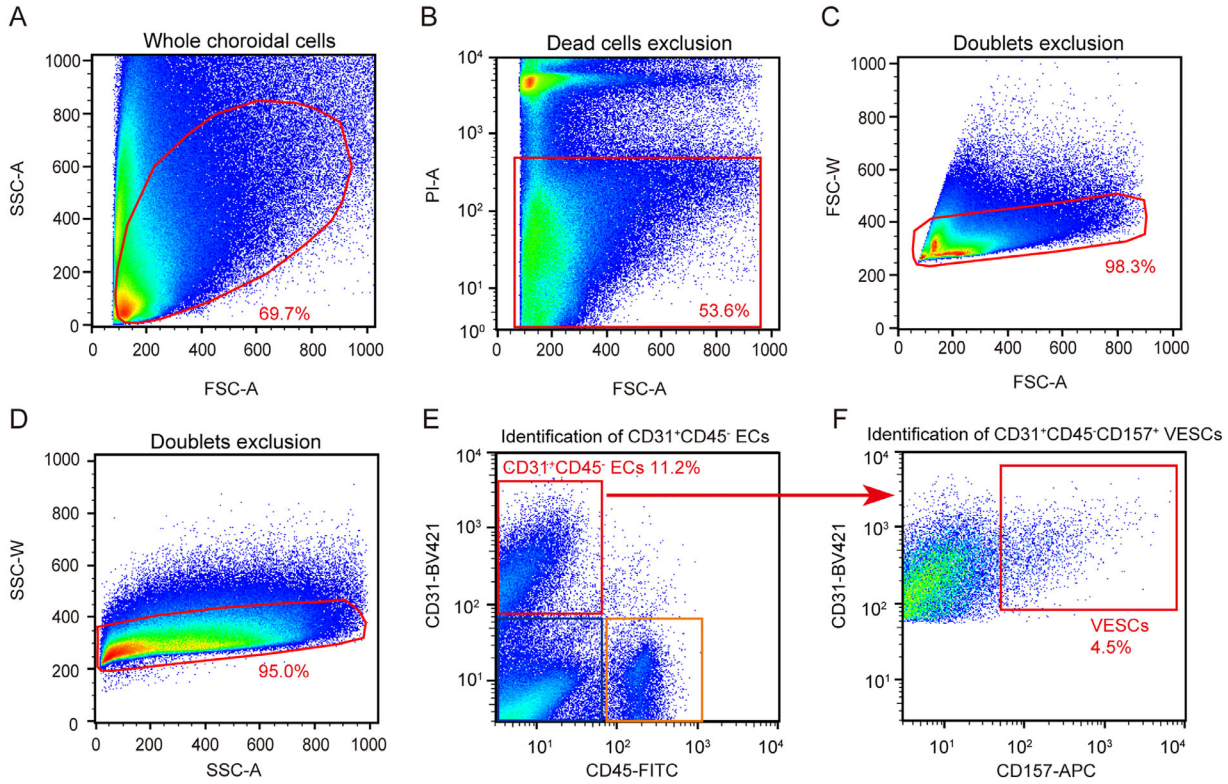

Figure 3. FACS gating strategy for sorting choroidal CD157-positive VESCs. Representative FACS plots of the percentage of parent gates for each population. The choroidal cell population was selected (**A**), dead cells were excluded (**B**), and doublets were excluded (**C, D**). (**E**) CD31-BV421-A versus CD45-FITC-A dot plot was generated to identify vascular ECs positive for the endothelial marker CD31 and negative for the hematopoietic marker CD45 ($CD31^+CD45^-$) in the choroid. The proportion of choroidal endothelial cells (ECs) shown in red squares was 9.2% in this experiment. The orange square shows hematopoietic cells ($CD31^+CD45^-$), and the blue squares indicate others ($CD31^-CD45^-$). (**F**) CD31-BV421-A versus CD157-APC-A dot plot was generated to detect CD157-positive vascular endothelial stem cells (VESCs). The proportion of VESCs was 4.3% among all choroidal ECs.

Olympus IX-70. The EC network area was measured using ImageJ software (National Institutes of Health, Bethesda, MD, USA). The EC network area was defined as the ratio of the CD31-positive area to the total area in each field.

Immunostaining the Whole-Mount Retina and Choroid

Enucleated eyes from 8-week-old C57BL/6J mice were fixed for 30 minutes in 4% paraformaldehyde (PFA) in PBS and then dissected. Retinal cups were removed before immunostaining the whole-mount retina. To whole-mount immunostain the choroid, the RPE/choroid/sclera complex was additionally fixed with 4% PFA for 30 minutes, and the RPE was removed by gentle brushing, resulting in a choroid/sclera complex. The retinal cups and choroid/sclera complexes were stained with primary antibodies, including rat monoclonal anti-CD31 (1:200, BD, cat. #553370) and PE anti-mouse CD157 antibody (clone BP-3, BioLegend, cat. #140204). The secondary antibody used was Alexa Fluor 647-conjugated goat anti-Rat IgG (H+L) (1:500, Thermo Fisher, cat. #A21247).

Statistical Analysis and Graphing

All data were presented as mean ± SEM. Statistical analyses were performed using Statcel 3 software (OMS, Tokorozawa, Japan). Data were compared using a Student's *t*-test. Statistical significance was set at $P < 0.05$. All graphs were generated using Excel and Adobe Illustrator CS6 software.

Results

Flow Cytometric Analysis of Retinal and Choroidal Cells

Single-cell suspensions were successfully prepared using retina and choroid samples. The CD31-BV421 versus CD45-FITC dot plot of retinal cells showed 3 fractions: (1) retinal ECs defined as positive for the endothelial marker CD31 and negative for the hematopoietic marker CD45 ($CD31^+CD45^-$); (2) hematopoietic cells ($CD31^-CD45^+$) such as macrophages; and (3) others ($CD31^-CD45^-$) such as photoreceptors, bipolar cells, and pericytes (see Fig. 2E). The fraction of retinal ECs represented 3.3 ± 0.1% based on total events in the retinal flow cytometry. Similarly, the CD31-BV421 versus CD45-FITC dot plot of choroidal cells showed 3 fractions: (1) choroidal ECs ($CD31^+CD45^-$); (2) hematopoietic cells ($CD31^-CD45^+$) such as macrophages; and (3) others ($CD31^-CD45^-$) such as RPEs (see Fig. 3E). The fraction of choroidal ECs was 11.5 ± 0.6% of the total events in the choroidal flow cytometry.

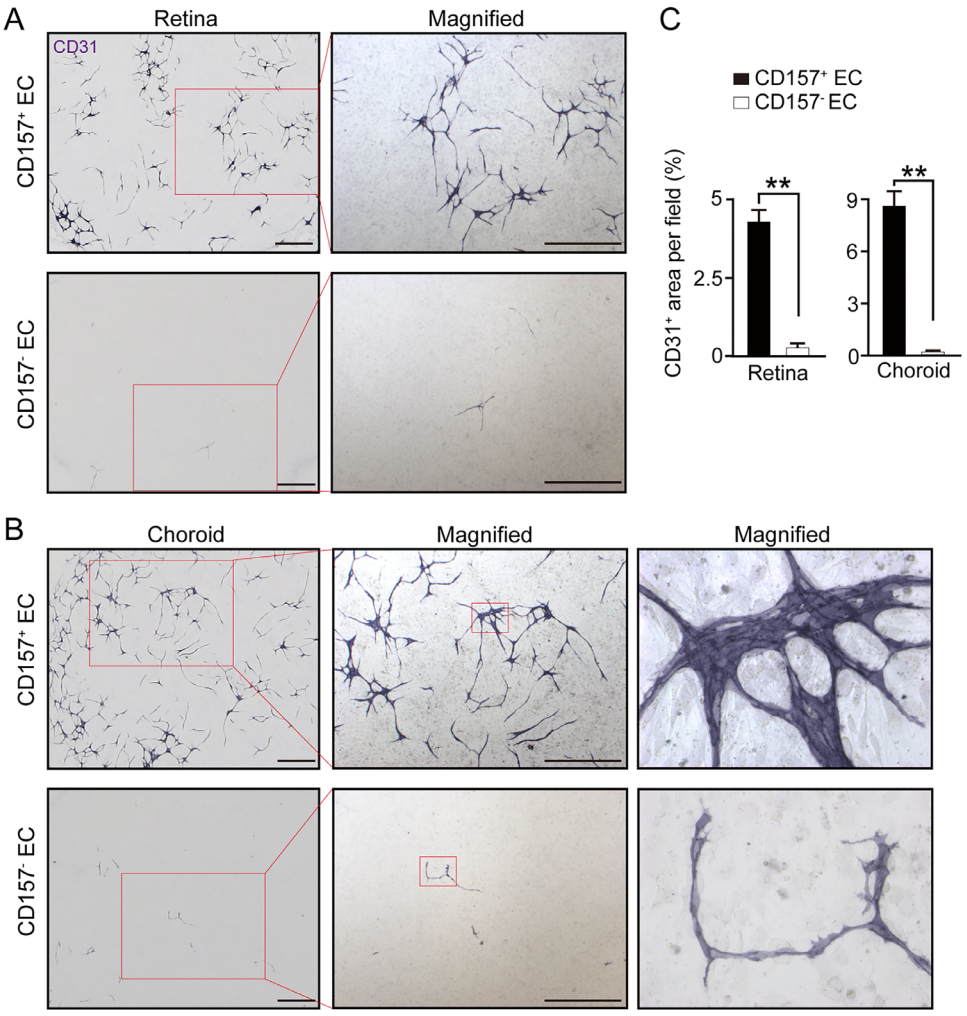

Figure 4. In vitro culture of CD157-positive VESCs showing proliferation and endothelial network formation. (**A**) CD157-positive VESCs and CD157-negative non-VESCs from the retina were cultured on OP9 feeder cells for 10 days. The cells were stained with an anti-CD31 antibody. Scale bars, 1 mm. (**B**) CD157-positive VESCs and CD157-negative non-VESCs from the choroid were cultured on OP9 feeder cells for 10 days. The cells were stained with an anti-CD31 antibody. Scale bars, 1 mm. (**C**) Quantification of the EC network area. $^{**}P < 0.01$, Student's *t*-test. Data are mean ± SEM ($n = 4$).

Identification and Isolation of CD157-Positive VESCs in the Retina and Choroid

In the retina, among $CD31^+CD45^-$ ECs, 1.6 ± 0.1% were CD157-positive VESCs ($CD31^+CD45^-$ $CD157^+$ ECs; see Fig. 2F). In the choroid, among $CD31^+CD45^-$ ECs, 4.5 ± 0.2% were CD157-positive VESCs (see Fig. 3F).

In Vitro Culture of VESCs

To evaluate the proliferative capacity of VESCs in vitro, sorted VESCs isolated from the retina and choroid were cultured on OP9 stromal cells that support EC growth. After 10 days, the CD157-positive VESCs isolated from the retina and choroid generated a higher number of EC networks compared with the CD157-negative non-VESCs (Fig. 4). The EC networks generated from VESCs contained multiple ECs. The endothelial network area, defined as the ratio of the CD31-positive area to the total area in each field, was 4.21 ± 0.39% in retinal VESCs and 0.27 ± 0.12% in retinal non-VESCs ($P < 0.01$). The endothelial network area was 8.59 ± 0.78% in choroidal VESCs and 0.14 ± 0.04% in choroidal non-VESCs ($P < 0.01$).

Location of VESCs

The immunostaining of retinal and choroidal blood vessels with CD31 and CD157 showed that CD157-positive VESCs were found in large blood vessels but not in the capillaries of both the retina and choroid (Fig. 5A, Fig. 6A). CD157 positive ECs were not detected in the retinas and choroids of the CD157-KO mice (Fig. 5B, Fig. 6B), indicating that the CD157 antibody used in the immunostaining specifically recognized CD157 in wild-type mouse vasculature. The CD157-positive cells were rarely found in the $CD31^-CD45^-$ fraction containing pericyte populations in the FACS analysis of wild-type mouse retina and choroid (Supplementary Fig. S2). Therefore, most of the CD157-positive cells immunostained in the retinal and choroidal vasculature were ECs that lined the blood vessels.

Investigative Ophthalmology & Visual Science

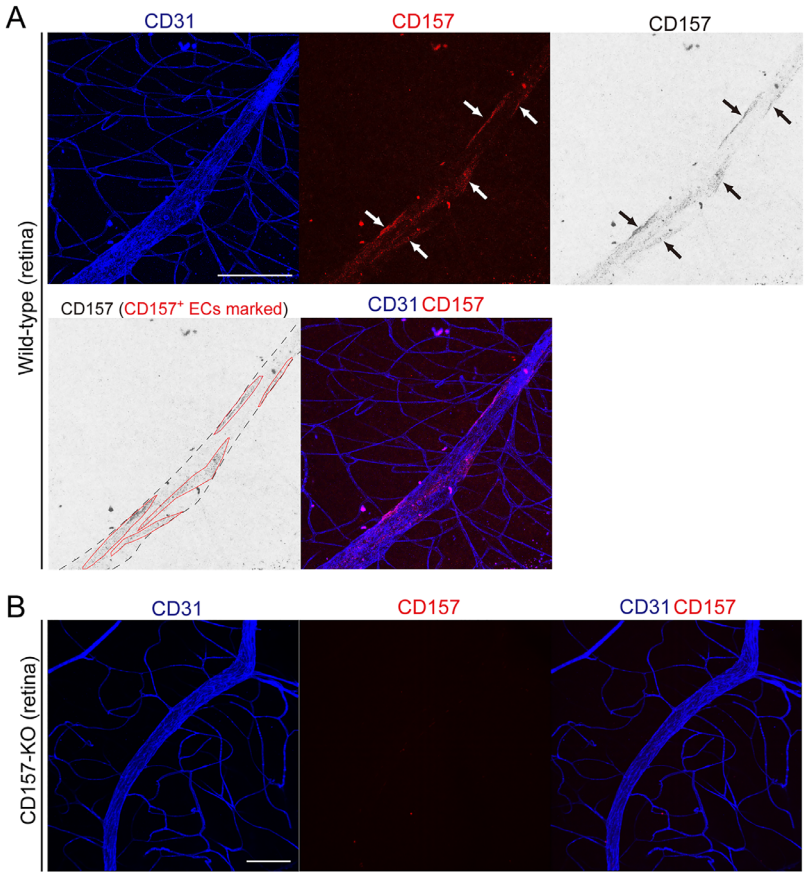

Figure 5. CD157 expressed in vascular endothelial cells (ECs) of large retinal vessels. (**A**) CD31 (*blue*) and CD157 (*red*) were stained using the retinal flat mount of a wild-type mouse. CD157-positive ECs were located in the large veins in the retina, but not in the capillaries. Scale bar represents 100 µm. (**B**) CD157 positive ECs were not detected in the retinas of CD157-KO ($CD157^{-/-}$) mouse, indicating that the CD157 antibody used in **A** specifically recognized CD157 in retinal vasculature. Scale bar represents 100 µm.

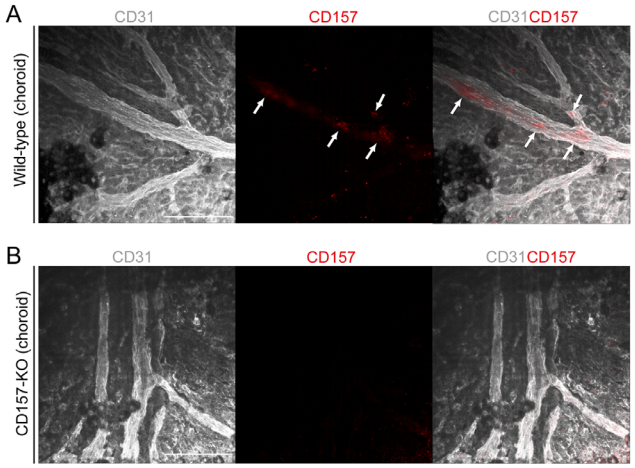

Figure 6. CD157 expressed in the vascular endothelial cells (ECs) of large choroidal vessels. (**A**) CD31 (*white*) and CD157 (*red*) were stained using the choroidal flat mount of a wild-type mouse. CD157-positive ECs were located in the large vessels in the choroid, but not in the capillaries. Scale bars represents 100 µm. (**B**) CD157 positive ECs were not detected in the choroid of CD157-KO ($CD157^{-/-}$) mice, indicating that the CD157 antibody used in **A** specifically recognized CD157 in choroidal vasculature. Scale bars represents 100 µm.

Discussion

In the current study, we established a protocol for creating a single-cell suspension and isolating vascular ECs from the retina and choroid. Using this protocol, we confirmed the distinct population of CD157-positive VESCs in mouse retina and choroid. The proportion of VESCs among the ECs was 1.6% in the retina and 4.5% in the choroid. In a previous study, we identified CD157-positive VESCs in most mouse organs, such as the brain, lungs, liver, heart, limb muscle, aorta, and inferior vena cava.[18,20] The proportions ranged from 2.7% to 14.9%. It is noteworthy that despite the different tissue-specific roles of the blood vessels in each organ, VESCs were specifically present in a small subset of vascular ECs, and a certain proportion in most organs expressed the common marker CD157 (Bst1). However, we did not elucidate why the CD157 molecule marked the VESCs. The CD157 antigen, which was originally identified as a BM stromal cell molecule (BST-1), facilitates pre-B cell growth. It is a glycosyl-phosphatidylinositol (GPI)-anchored membrane protein that is considered to act independently as an enzyme and receptor.[21–23] As an enzyme, CD157 exerts ADP ribosyl cyclase and cyclic ADP-ribose (cADPR) hydrolase activities (metabolism of NAD+).[24] NAD+ is important for stem cell activity in muscle stem cells.[25] As a receptor, CD157 initiates an intracellular signal transduction cascade, resulting in the

phosphorylation of focal adhesion kinase and Src, leading to the activation of downstream MAPK/ERK and PI3K/Akt signaling pathways that regulate cell adhesion, migration, and survival.[21] Although CD157 may, in part, influence the ability of VESCs, we did not identify any apparent abnormalities or defects in the blood vessels or proliferative ability of VESCs in CD157-KO mice in both a previous study[18] and the present study. Therefore, the genes that define the key functional features of VESCs are still obscure and should be explored in future studies.

The in vitro cultures in the present study clearly showed a higher proliferative capacity of CD157-positive VESCs in the retina and choroid compared with most ECs that did not express CD157. A previous study showed that VESCs strongly expressed transcriptional factors known to regulate cellular differentiation and proliferation, such as Myc, Fosl2, ATF3, Foxp1, and Sox7.[18] ABC transporters, such as ABCG2, ABCB1a, and ABCC4, which may affect the proliferative potential, were also highly expressed in VESCs.[17,18] These genes may be responsible for the higher proliferative capacity of CD157-positive VESCs.

In this study, CD157-positive VESCs were located in the large blood vessels in the retina and choroid, but not in the capillaries. Our previous study also showed that CD157-positive VESCs were principally present in large blood vessels, especially in veins in the liver, lungs, and heart.[18] Recent single-cell RNA sequencing of lung ECs and choroidal ECs showed that genes that are highly expressed in VESCs, such as CD157, ABCG2, ABCB1a, and ABCC4, are highly expressed in ECs in veins and post-capillary venules (PCVs).[26,27] In other words, VESCs are located predominantly in the veins and PCVs among heterogenous vascular trees, including arteries, arterioles, capillaries, PCVs, and veins. A study on single-cell RNA sequencing also showed that the hierarchy of vascular ECs originates in veins that express VESCs markers and differentiates into PCVs and then further into an immature vascular EC phenotype, including tip cells, neophalanx, and activated arteries.[26,27] An early histopathological study suggested that vessel sprouting (angiogenesis) originates in the veins and PCVs.[28,29] Our study not only identified VESCs in the retina and choroid but also suggested that the VESCs present in veins and PCVs have specific molecular and functional characteristics that are responsible for angiogenesis. These specific characteristics may explain why angiogenesis is initiated in specific locations, such as veins and PCVs, as reported in early histopathological studies.[28,29]

This study has the following limitations. We used the term VESCs to refer to CD157-positive ECs in the retina and choroid, as single CD157-positive ECs had stem cell properties that included homeostatic capillary maintenance and regenerative capacity upon vascular injury in vivo in the liver.[18] However, we could not determine in vivo evidence of the contribution of CD157-positive VESCs to the physiological turnover of capillaries or the initiation of angiogenesis in the retina and choroid. Thus, the data shown here do not signify that CD157-positive ECs in the retina and choroid are true stem cells that can maintain vasculature and regenerate retinal and choroidal vessels in vivo. In future research, fate-mapping analysis of CD157-positive ECs using the CD157-CreERT mouse line could provide direct evidence of the regenerative capacity of retinal and choroidal CD157-positive VESCs. In addition, further studies are needed to elucidate whether a single marker, CD157 alone, characterizes VESCs or whether additional markers may more effectively identify, isolate, or characterize true stem cell populations.

Elucidating the molecular mechanism of VESC proliferation could support the use of vascular regeneration therapy for ischemic retinal diseases and vascular aging. Our previous study suggested that VESCs not only maintain physiological vasculature but also potentially contribute to pathological neovascularization, such as tumor angiogenesis and choroidal neovascularization.[17,30] Therefore, it would be fruitful to determine whether VESCs are responsible for initiating retinal and choroidal neovascularization in pathological conditions, such as hypoxia and inflammation. This evidence could lead to the development of new antiangiogenic therapies for diabetic retinopathy, retinopathy of prematurity, and age-related macular degeneration.

In summary, we confirmed the existence and proliferative ability of VESCs in the large blood vessels of mouse retina and choroid. Future studies are necessary to reveal the molecular mechanism of the role of CD157-positive VESCs in physiological maintenance and pathological angiogenesis. Fate-mapping analysis of CD157-positive VESCs could be a powerful tool for clarifying the role of VESCs in vivo. Furthermore, the potential existence of VESCs in humans should be investigated in future research.

Acknowledgments

Supported by Grant-in-Aid for Young Scientists (B) (16K20317) and the Japan Agency for Medical Research and Development (AMED), Precursory Research for Innovative Medical Care (PRIME; 21gm6210009h0004), JSPS KAKENHI (20H03435), the Takeda Science Foundation, and the Mochida Memorial Foundation for Medical and Pharmaceutical Research.

Disclosure: **T. Wakabayashi**, None; **H. Naito**, None; **T. Iba**, None; **K. Nishida**, None; **N. Takakura**, None

References

1. Yu DY, Cringle SJ. Oxygen Distribution and Consumption within the Retina in Vascularized and Avascular Retinas and in Animal Models of Retinal Disease. *Prog Retin Eye Res*. 2001;20(2):175–208.
2. Wangsa-Wirawan ND, Linsenmeier RA. Retinal Oxygen: Fundamental and Clinical Aspects. *Arch Ophthalmol-Chic*. 2003;121(4):547–557.
3. Benedicto I, Lehmann GL, Ginsberg M, et al. Concerted regulation of retinal pigment epithelium basement membrane and barrier function by angiocrine factors. *Nat Commun*. 2017;8(1):15374.
4. Paredes I, Himmels P, de Almodóvar CR. Neurovascular Communication during CNS Development. *Dev Cell*. 2018;45(1):10–32.
5. Potente M, Gerhardt H, Carmeliet P. Basic and Therapeutic Aspects of Angiogenesis. *Cell*. 2011;146(6):873–887.
6. Grant MB, May WS, Caballero S, et al. Adult hematopoietic stem cells provide functional hemangioblast activity during retinal neovascularization. *Nat Med*. 2002;8(6):607–612.
7. Asahara T, Murohara T, Sullivan A, et al. Isolation of Putative Progenitor Endothelial Cells for Angiogenesis. *Science*. 1997;275(5302):964–966.
8. Naito H, Iba T, Takakura N. Mechanisms of new blood-vessel formation and proliferative heterogeneity of endothelial cells. *Int Immunol*. 2020;32(5):295–305.
9. Okuno Y, Nakamura-Ishizu A, Kishi K, Suda T, Kubota Y. Bone marrow-derived cells serve as proangiogenic

macrophages but not endothelial cells in wound healing. *Blood*. 2011;117(19):5264–5272.
10. Palma MD, Venneri MA, Roca C, Naldini L. Targeting exogenous genes to tumor angiogenesis by transplantation of genetically modified hematopoietic stem cells. *Nat Med*. 2003;9(6):789–795.
11. Grunewald M, Avraham I, Dor Y, et al. VEGF-Induced Adult Neovascularization: Recruitment, Retention, and Role of Accessory Cells. *Cell*. 2006;124(1):175–189.
12. McDonald AI, Shirali AS, Aragón R, et al. Endothelial Regeneration of Large Vessels Is a Biphasic Process Driven by Local Cells with Distinct Proliferative Capacities. *Cell Stem Cell*. 2018;23(2):210–225.e6.
13. Mondor I, Jorquera A, Sene C, et al. Clonal Proliferation and Stochastic Pruning Orchestrate Lymph Node Vasculature Remodeling. *Immunity*. 2016;45(4):877–888.
14. Ingram DA, Mead LE, Tanaka H, et al. Identification of a novel hierarchy of endothelial progenitor cells using human peripheral and umbilical cord blood. *Blood*. 2004;104(9):2752–2760.
15. Banno K, Yoder MC. Tissue regeneration using endothelial colony-forming cells: promising cells for vascular repair. *Pediatr Res*. 2018;83(1-2):283–290.
16. Naito H, Kidoya H, Sakimoto S, Wakabayashi T, Takakura N. Identification and characterization of a resident vascular stem/progenitor cell population in preexisting blood vessels. *Embo J*. 2012;31(4):842–855.
17. Wakabayashi T, Naito H, Takara K, et al. Identification of Vascular Endothelial Side Population Cells in the Choroidal Vessels and Their Potential Role in Age-Related Macular Degeneration SP Cell in the Choroid. *Invest Ophth Vis Sci*. 2013;54(10):6686–6693.
18. Wakabayashi T, Naito H, Suehiro J ichi, et al. CD157 Marks Tissue-Resident Endothelial Stem Cells with Homeostatic and Regenerative Properties. *Cell Stem Cell*. 2018;22(3):384–397.e6.
19. Itoh M, Ishihara K, Hiroi T, et al. Deletion of bone marrow stromal cell antigen-1 (CD157) gene impaired systemic thymus independent-2 antigen-induced IgG3 and mucosal TD antigen-elicited IgA responses. *J Immunol*. 1998;8(161):3974–3983.
20. Naito H, Wakabayashi T, Ishida M, et al. Isolation of tissue-resident vascular endothelial stem cells from mouse liver. *Nat Protoc*. 2020;15(3):1066–1081.
21. Ortolan E, Augeri S, Fissolo G, Musso I, Funaro A. CD157: from immunoregulatory protein to potential therapeutic target. *Immunol Lett*. 2018;205:59–64.
22. Kaisho T, Ishikawa J, Oritani K, et al. BST-1, a surface molecule of bone marrow stromal cell lines that facilitates pre-B-cell growth. *Proc National Acad Sci*. 1994;91(12):5325–5329.
23. Itoh M, Ishihara K, Tomizawa H, et al. Molecular Cloning of Murine BST-1 Having Homology with CD38 and Aplysia ADP-Ribosyl Cyclase. *Biochem Bioph Res Co*. 1994;203(2):1309–1317.
24. Hirata Y, Kimura N, Sato K, et al. ADP ribosyl cyclase activity of a novel bone marrow stromal cell surface molecule, BST-1. *Febs Lett*. 1994;356(2-3):244–248.
25. Zhang H, Ryu D, Wu Y, et al. NAD^+ repletion improves mitochondrial and stem cell function and enhances life span in mice. *Science*. 2016;352(6292):1436–1443.
26. Goveia J, Rohlenova K, Taverna F, et al. An Integrated Gene Expression Landscape Profiling Approach to Identify Lung Tumor Endothelial Cell Heterogeneity and Angiogenic Candidates. *Cancer Cell*. 2020;37(1):21–36.e13.
27. Rohlenova K, Goveia J, García-Caballero M, et al. Single-Cell RNA Sequencing Maps Endothelial Metabolic Plasticity in Pathological Angiogenesis. *Cell Metab*. 2020;31(4):862–877.e14.
28. Folkman J. Angiogenesis: Initiation and Control*. *Ann NY Acad Sci*. 1982;401(1):212–226.
29. Ishibashi T, Miller H, Orr G, Sorgente N, Ryan SJ. Morphologic observations on experimental subretinal neovascularization in the monkey. *Invest Ophth Vis Sci*. 1987;28(7):1116–1130.
30. Naito H, Wakabayashi T, Kidoya H, et al. Endothelial Side Population Cells Contribute to Tumor Angiogenesis and Antiangiogenic Drug Resistance. *Cancer Res*. 2016;76(11):3200–3210.

Investigative Ophthalmology & Visual Science